

LATERAL LOAD BEARING CHARACTERISTICS OF LIGHT GAUGE STEEL AND LIGHTWEIGHT CONCRETE SHEAR WALLS

CHUNRI QUAN^{a,*}, QIANG HUANG^b, DONGBIN LI^c, YONG CHEN^d

^a Osaka Institute of Technology, Department of Architecture, 5-16-1 Omiya, Asahi-ku, 535-8585 Osaka, Japan

^b China BIM Union, Department of Management, No.30 Beisanhuandonglu, 100013 Beijing, China

^c China Building Technique Group Co., Ltd., Engineering Technology Research Center, No.30 Beisanhunadonglu, 100013 Beijing, China

^d ARSE Building Engineering Technology Co., Ltd., Design Department, No.365 Dongsihuannanlu, 100023 Beijing, China

* corresponding author: chunri.quan@oit.ac.jp

ABSTRACT.

In China, there is a new structural system named light gauge steel and lightweight concrete (LSLC) structure, which used lightweight concrete as structural material in composite way with cold-formed steel. Here, the shear walls are the main structural members for the LSLC structure, which are assembled with the light gauge steel lattice columns and horizontal braces, and filled with lightweight concrete. In this study, the LSLC shear walls are experimentally investigated to evaluate their failure mechanism and lateral load bearing capacity. For this purpose, several specimens with different shear span ratio are designed and tested under static cyclic loading. This paper presents the damage state and hysteresis loops of the specimens detailly. Then, the lateral load bearing characteristics of the LSLC shear walls are discussed according to the failure mechanism, such as shear and flexural failure. Finally, the calculation methods of lateral strength for the LSLC shear walls are proposed based on the diagonal strut mechanism and sectional force equilibrium.

KEYWORDS: Failure mechanism, lateral load bearing characteristic, light gauge steel and lightweight concrete structure, shear wall.

1. INTRODUCTION

Cold-formed steel structure has been widely used in the low-rise buildings due to its high strength, ease of construction, and low cost [1]. On the other hand, due to low self-weight, good workability, excellent performance on thermal insulation, fire resistance and sound absorption, lightweight concrete was primarily utilized as non- and semi-structural material in the past building construction [2]. Motivated by the industrialized performance of cold-formed steel structure, good integrity of cast-in-situ concrete structure and advantages of the lightweight concrete, a new structure system named light gauge steel and lightweight concrete (LSLC) structure, which used expanded polystyrene concrete or foamed concrete as the structural material in composite way with the cold-formed steel, was proposed and applied to the building construction in China [3]. Compared with the traditional reinforced concrete structure, the LSLC structure can reduce seismic load significantly based on the use of lightweight concrete to decrease the self-weight of overall structure. Compared with the cold-formed steel structure, the LSLC structure has great advantages in features such as fire protection, thermal insulation and sound absorption.

In the past several years, the studies of the LSLC structure were focused on the members such as shear

walls and slabs, furthermore their design method has been developed based on the considerable tests. This paper describes the design details and testing method for the LSLC shear wall specimens, with different shear span ratio as the experimental parameters. Then, the damage state and hysteresis loops of specimens are presented detailly, and the seismic capacity of the LSLC shear wall is evaluated based on the cyclic lateral loading test results. Finally, the lateral load bearing characteristics of the LSLC shear walls are discussed, and the calculation methods of lateral strength for the LSLC shear walls are proposed.

2. OUTLINE OF EXPERIMENT

2.1. CONFIGURATION OF THE LSLC SHEAR WALL

Shear wall is the main structural member of the LSLC structure system. Figure 1 shows the standard configuration of the shear wall with thickness of 180mm and concrete cover thickness of 20mm. Light gauge steel frame is assembled with the light gauge steel lattice columns and horizontal braces, then filled with lightweight concrete. The lattice columns composed of two or four square steel tubes, which were combined and fixed by batten plates and bolts with 600 mm spacing as shown in Figure 2. Steel strips with

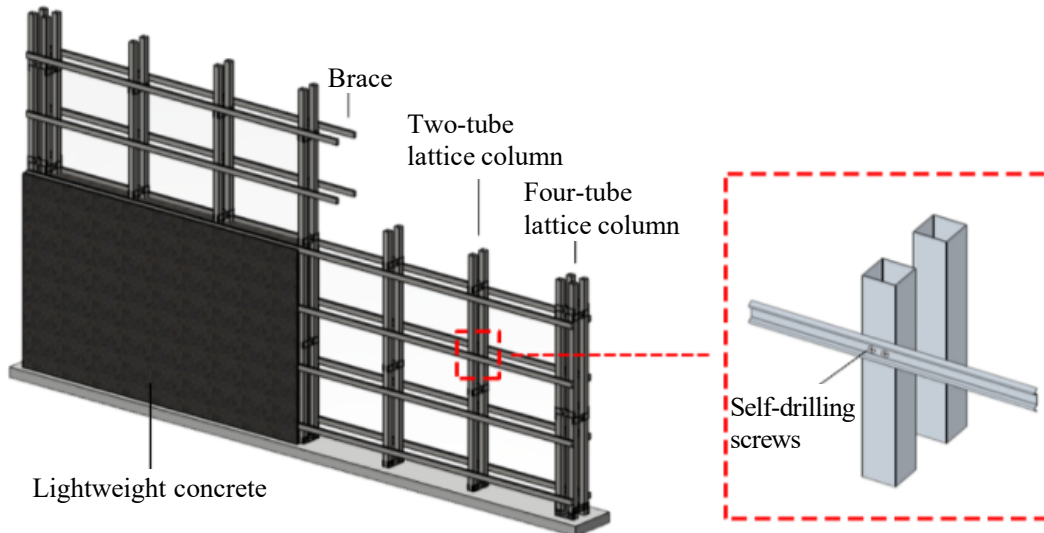


FIGURE 1. Configuration of the LSLC shear wall.

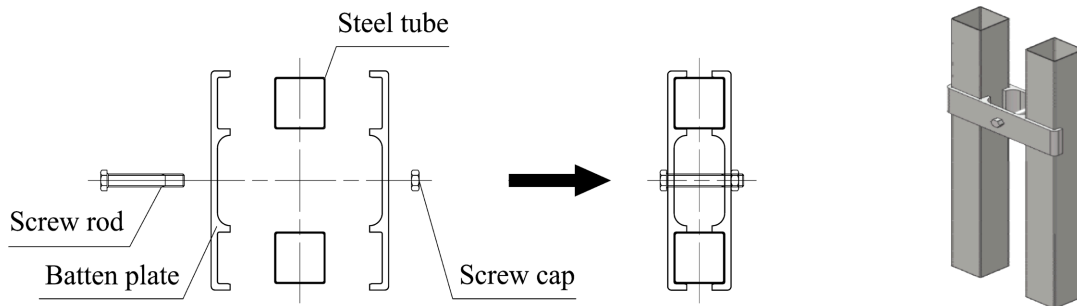


FIGURE 2. Installation of batten plates in the lattice column.

Specimen	Height × Width × Thickness (mm)	Shear span ratio	Axial force ratio
S0.8-A0.4	1650 × 2062.5 × 180	0.8	0.4
S1.5-A0.4	2250 × 1500 × 180	1.5	0.4
S2.5-A0.4	2250 × 900 × 180	2.5	0.4

TABLE 1. Experiment parameters.

W-shaped cross section were installed as horizontal braces with spacing of 600mm, which were connected to the lattice columns by self-drilling screws.

2.2. DESIGN OF SPECIMEN

The test specimens are designed according to the standard design method of LSLC shear wall mentioned above. In this study, five full-scale specimens with different shear span ratio and axial force ratio as the experimental parameters are tested under in-plain cyclic loadings.

Table 1 and Figure 3 show the experiment parameters and design details of specimens. The light gauge steel lattice columns of each specimen are composed of four and two square steel tubes at the side and the middle of the wall, respectively. Then, the lattice columns are anchored in the reinforced concrete rigid beam (stub). The horizontal braces are installed with

spacing of 600mm, which are connected to the lattice columns by three self-drilling screws.

2.3. MATERIAL CHARACTERISTIC

Table 2 and table 3 show the material test results, where the values represent the mean value of 3 samples in each test. The light gauge steel is designated as S350GD conform to the Chinese National Standard GB/T2518 [4]. which requires the yield strength and tensile strength not less than 350MPa and 420 MPa, respectively. In addition, No.4.8 self-drilling screw given in the ISO15481 [5] is adopted as fastener.

The expanded polystyrene concrete with design-ing density of 1000kg/m³ is used as lightweight concrete. Here, test samples with dimensions 100 mm × 100 mm × 100 mm are prepared in casting process of each specimen, then the compressive strength and density are measured according to the Chinese National Standard GB/T50080 [6].

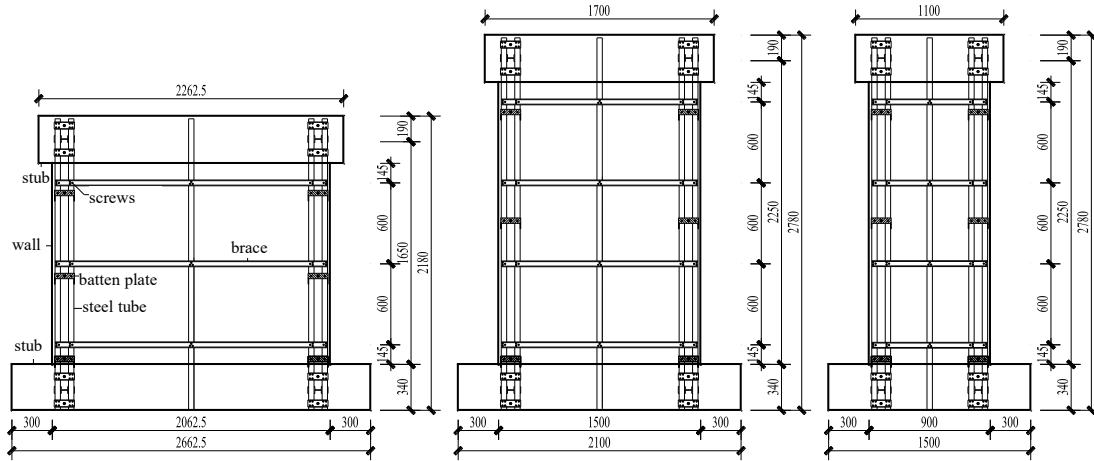


FIGURE 3. Details of specimens (unit: mm).

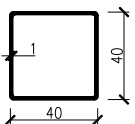
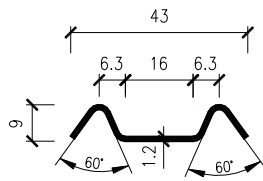
Member	Yield strength [MPa]	Tensile strength [MPa]	Young's modulus [MPa]	Cross-section [mm]
Lattice column	361.5	484.3	2.02×10^5	
Horizontal brace	352.1	462.2	1.98×10^5	

TABLE 2. Mechanical properties and cross-section size of light gauge steel.

Density [kg/m ³]	Compressive strength [MPa]	Young's modulus [MPa]
1058	6.36	0.72×10^4

TABLE 3. Mechanical properties of lightweight concrete (expanded polystyrene concrete).

2.4. LOADING PROGRAM

The loading system and history are shown in Figure 4 and Figure 5, respectively. The lateral cyclic loading is performed by load control system until the yielding of light gauge steel. Then, it is switched to displacement control, and peak drift angles (the ratio of lateral deformation to wall height) are planned by the times of displacement (Δ) when the light gauge steel is yielded. Here, two cycles for each peak drift are imposed. The axial load is applied to each specimen based on the axial force ratio.

3. TEST RESULTS

3.1. FAILURE PATTERNS

Figure 6 shows the crack patterns in each specimen at the safety limitation, where it is defined as the

moment in which the maximum lateral strength of the LSLC shear wall deteriorates to its 85%.

3.1.1. S0.8-A0.4 SPECIMEN

A shear crack at the middle of wall is observed at the drift angle of 0.11% with the width of 0.15mm. Loaded to 0.25%, some vertical cracks occur at the upper of wall along the light gauge steel lattice columns. At the drift angle of 1.88%, clear shear cracks are observed at the diagonal of wall.

3.1.2. S1.5-A0.4 SPECIMEN

A shear crack at the bottom of wall is observed at the drift angle of 0.11% with the width of 0.1mm. Loaded to 0.36%, some vertical cracks and flexural cracks occur in succession. At the drift angle of 3.02%, the vertical cracks and flexural cracks continue to extend and the width increases.

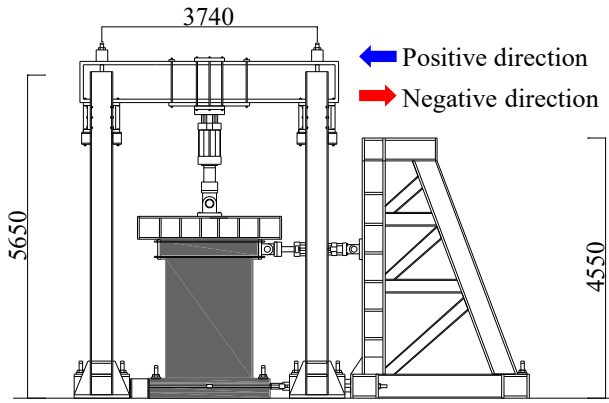


FIGURE 4. Test setup (unit: mm).

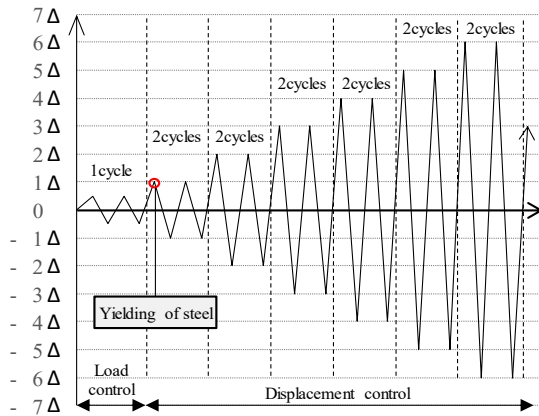


FIGURE 5. Loading history.

3.1.3. S2.5-A0.4 SPECIMEN

There are some flexural and flexural-shear cracks are observed at the drift angle of 0.21% with the maximum width of 0.15mm. Loaded to 0.34%, vertical and horizontal cracks occur along the light gauge steel lattice columns and braces. At the drift angle of 3.04%, the width of flexural cracks increases, and local crush of lightweight concrete cover is observed at the bottom of wall.

3.2. HYSTERETIC CHARACTERISTICS

Figure 7 shows the relationship between lateral strength and drift angle.

3.2.1. S0.8-A0.4 SPECIMEN

The maximum lateral strength of 295.5kN is recorded at the drift angle of 0.59%. Then, remarkably rapid strength deterioration is observed until the drift angle of 1.53%, which is the safety limitation of the specimen. It shows typical shear failure characteristics.

3.2.2. S1.5-A0.4 SPECIMEN

The maximum lateral strength of 146.2kN is recorded at the drift angle of 1.15%. Then, relatively slow strength deterioration is observed until the drift angle of 2.10%, which is the safety limitation of the specimen. It shows flexural-shear failure characteristics.

3.2.3. S2.5-A0.4 SPECIMEN

The maximum lateral strength of 73.8kN is recorded at the drift angle of 0.46%. Then, slow strength deterioration is observed until the drift angle of 1.23%, which is the safety limitation of the specimen. It shows typical flexural failure characteristics.

4. SEISMIC CAPACITY EVALUATION

4.0.1. LATERAL LOAD BEARING CAPACITY

Figure 8 shows the relationship between maximum lateral strength and shear span ratio. The maximum lateral strength decreases with the increase of the shear span ratio. Compared with the S0.8-A0.4 specimen, the maximum lateral strength of the S2.5-A0.4 specimen decreases by 75.0%. It can be considered that the flexural failure characteristics of shear wall gradually dominates with the increase of the shear span ratio.

4.1. DEFORMATION CAPACITY

Figure 9 shows the relationship between ductility coefficient and shear span ratio. Herein, the ductility coefficient (μ) of the LSLC shear wall is calculated as the ratio of failure displacement (Δ_u , displacement of safety limitation) to yield displacement (Δ_y), which is defined as shown in Figure 10. It is difficult to determine the internal relationship between the shear span ratio and the ductility coefficient of the LSLC shear wall. However, the ductility coefficient of each specimen is larger than 4, showing better deformation capacity compared with the reinforced concrete shear walls [7].

4.2. ENERGY ABSORPTION CAPACITY

Since the absolute value of dissipated energy depends on the scale of the specimen such as the cross-sectional area, the normalized equivalent damping ratio (h_{eq}) is applied to evaluate the energy absorption capacity of the LSLC shear wall. Herein, the equivalent damping ratio is calculated from the energy absorbed in one cycle (ΔW) and equivalent potential energy (W_e , strain energy) as shown in Figure 11.

Figure 12 shows equivalent damping ratio of each specimen. The maximum value of the equivalent damping ratio for each specimen is recorded 17.19 ~ 19.27%. After loading to the drift angle of 0.5%, the equivalent damping ratio of the LSLC shear wall shows the relatively stable values as 12 ~ 20%. Compared with the reinforced concrete shear walls [8], the LSLC shear walls show lower energy absorption capacity in this experimental study, and it can be considered that the severe slip of the LSLC shear wall reduced the hysteretic dissipated energy.

5. CALCULATION METHODS OF LATERAL STRENGTH

In this paper, the past experimental results of eleven specimens are employed to calculate the lateral

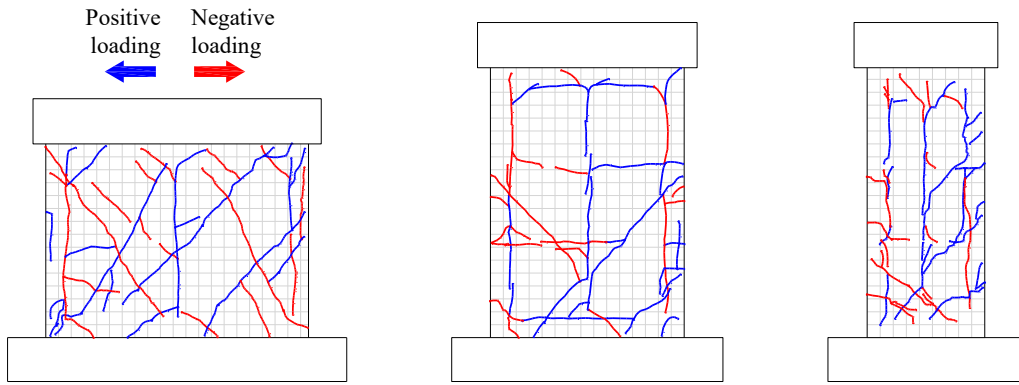


FIGURE 6. Crack patterns.

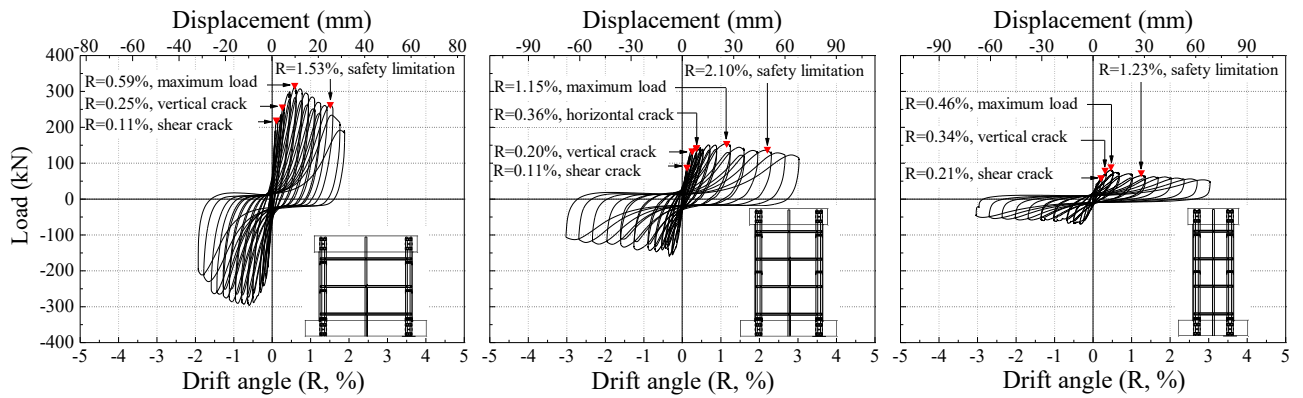


FIGURE 7. Lateral strength and drift angle relation.

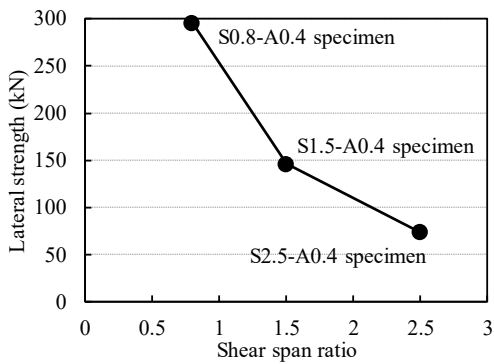


FIGURE 8. Maximum lateral strength.

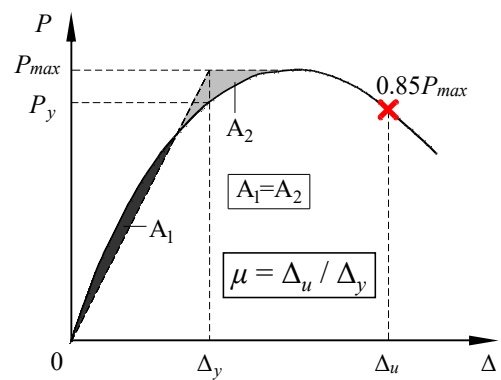


FIGURE 10. Characteristic points of $P - \Delta$ curve.

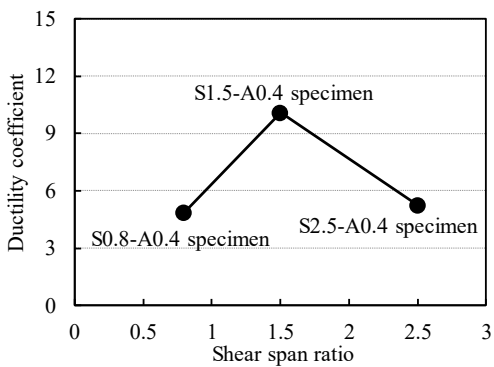


FIGURE 9. Ductility coefficient.

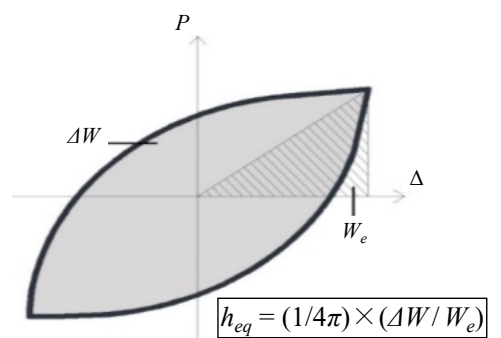


FIGURE 11. Definition of equivalent damping ratio.

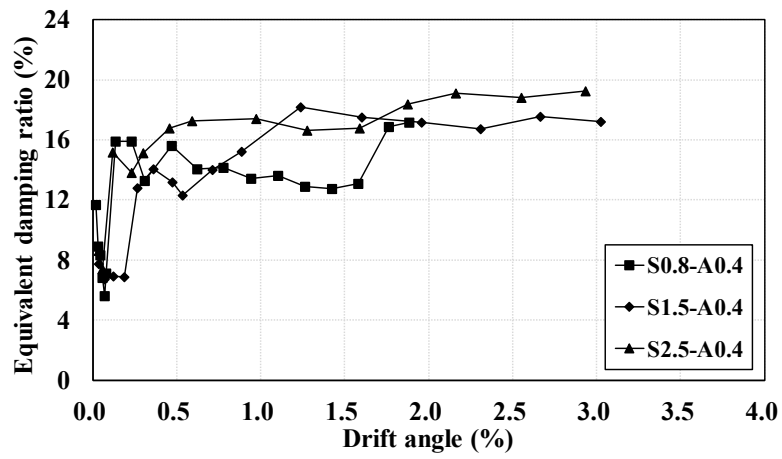


FIGURE 12. Equivalent damping ratio.

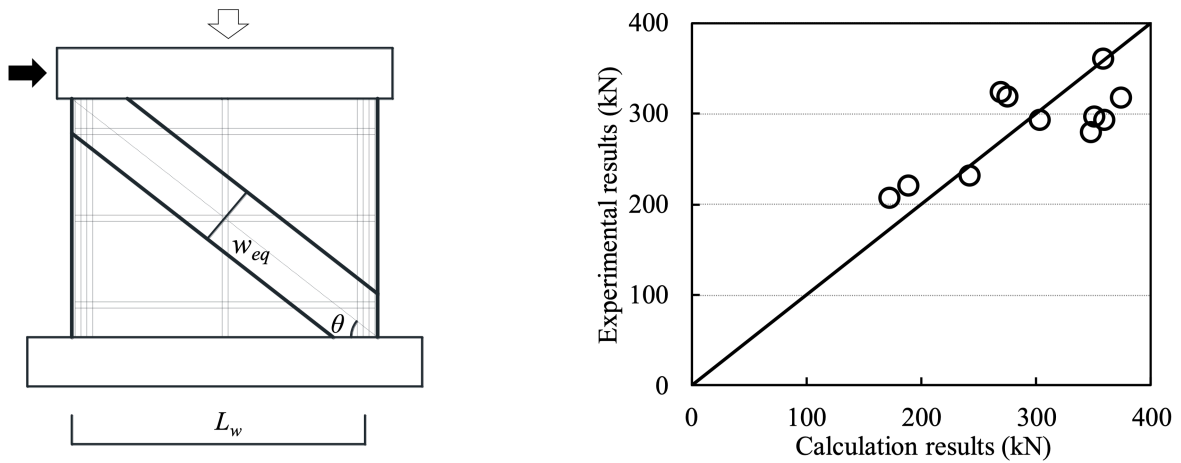


FIGURE 13. Concept and calculation results of diagonal strut mechanism.

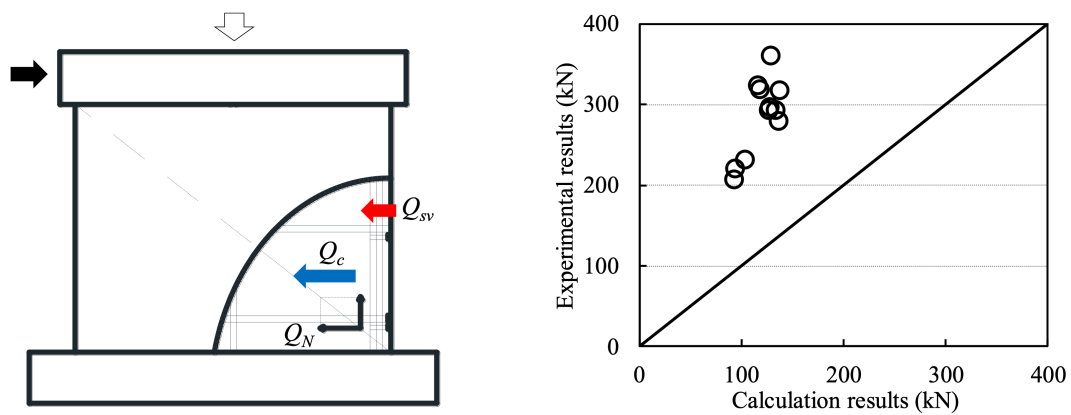


FIGURE 14. Concept and calculation results of sectional force equilibrium.

strength for the LSLC shear walls, which are showed shear failure [9].

5.0.1. DIAGONAL STRUT MECHANISM

The lateral strength Q_{su} for the LSLC shear walls could be calculated based on the diagonal strut mechanism, as shown in Equation 1, 2, and 3 [10]. Here, f_c is the compressive strength of lightweight concrete, w_{eq} is the equivalent strut width, t is the thickness of LSLC wall, θ is the strut angle to LSLC wall length, L_w is the length of LSLC wall, N_c is the axial force of lightweight concrete, A_c is the sectional area of lightweight concrete, σ_N is the compressive stress of LSLC wall, f_t is the tensile strength of lightweight concrete, respectively. As shown in Figure 13, the calculation results of the lateral strength for the LSLC shear wall based on the diagonal strut mechanism show good agreement with the experimental results.

$$Q_{su} = f_c w_{eq} t \cos \theta \quad (1)$$

$$w_{eq} = \left(0.25 + 0.85 \frac{N_c}{A_c f_c} \right) L_w \quad (2)$$

$$\theta = 90^\circ - \cos^{-1} \left[\left(\frac{\sigma_N}{\sigma_N + 2 f_t} \right) / 2 \right] \quad (3)$$

5.1. SECTIONAL FORCE EQUILIBRIUM

The lateral strength Q_{su} for the LSLC shear walls could be calculated based on the sectional force equilibrium, as shown in Equation 4, 5 [3]. Here, Q_c is the strength shared by lightweight concrete, Q_{sv} is the strength shared by horizontal brace, Q_N is the increased strength by axial force, λ is the shear span ratio of LSLC wall, f_t is the tensile strength of lightweight concrete, f_a is the tensile strength of light gauge steel, A_c is the sectional area of lightweight concrete, A_{ah} is the sectional area of horizontal brace, s is the space of horizontal brace, h_{w0} is the equivalent length of LSLC wall, N is axial force to LSLC wall, γ_{RE} is the seismic adjustment coefficient (here, 0.85), respectively. As shown in Figure 14, the calculation results of the lateral strength for the LSLC shear wall based on the sectional force equilibrium show conservative evaluation, compared with the experimental results.

$$Q_{su} = Q_c + Q_N + Q_{sv} \quad (4)$$

$$Q_{su} = \left[\frac{1}{\lambda - 0.5} (0.3 f_t A_c + 0.06 N) + 0.2 f_a \frac{A_{ah}}{s} h_{w0} \right] / \gamma_{RE} \quad (5)$$

6. CONCLUSIONS

Seismic performance of the light gauge steel and lightweight concrete shear wall was experimentally investigated under in-plane cyclic loadings. The major findings can be summarized as follows.

1. The effects of shear span ratio on the lateral load bearing capacity of the LSLC shear wall were grasped quantitatively.
2. The ductility coefficient of each specimen was larger than 4, showed better deformation capacity compared with the reinforced concrete shear walls. However, the equivalent damping ratio of the LSLC shear wall was calculated the values of 12 ~ 20%, showed lower energy absorption capacity compared with the reinforced concrete shear walls.
3. The lateral strength of the LSLC shear wall calculated based on the diagonal strut mechanism showed good agreement with the experimental results. However, the calculation based on the sectional force equilibrium showed conservative value compared with the experimental results.

ACKNOWLEDGEMENTS

The financial support of the Self-funded Project of China Academy of Building Research Co., Ltd (for Applied Technology Research, Grant No. 20151802330730055) is gratefully appreciated.

REFERENCES

- [1] N. Balh, J. DaBreo, C. Ong-Tone, et al. Design of steel sheathed cold-formed steel framed shear walls. *Thin-Walled Structures* **75**:76-86, 2014. <https://doi.org/10.1016/j.tws.2013.10.023>.
- [2] M. R. Jones, A. McCarthy. Preliminary views on the potential of foamed concrete as a structural material. *Magazine of Concrete Research* **57**(1):21-31, 2005. <https://doi.org/10.1680/macr.2005.57.1.21>.
- [3] Ministry of housing and urban-rural development. Technical specification of lightweight steel and lightweight concrete structure China, 2016.
- [4] Chinese National Standard. Continuously hot-dip zinc-coated steel sheet and strip, *Beijing: Standards Press of China*, 2008.
- [5] International Standards Organization. Cross recessed pan head drilling screws with tapping screw thread, 1999.
- [6] Chinese National Standard (GB/T50080). Standard for test method of performance on ordinary fresh concrete, *Beijing: Architecture Industrial Press of China*, 2001.
- [7] T. Shimazu, Y. Fukuhara, T. Satoh T, et al. New reinforced concrete structure Japan, 2002.
- [8] H. Tomatsuri. *Proceedings of the Japan Concrete Institute* **31**(2):409-14.
- [9] China Building Technique Group Co., Ltd. An experimental report of light gauge steel and lightweight concrete shear walls Beijing, 2015.
- [10] S.-J. Hwang, W.-H. Fang, H.-J. Lee, et al. Analytical Model for Predicting Shear Strength of Squat Walls. *Journal of Structural Engineering* **127**(1):43-50, 2001. [https://doi.org/10.1061/\(asce\)0733-9445\(2001\)127:1\(43\)](https://doi.org/10.1061/(asce)0733-9445(2001)127:1(43)).